

PALEOSEISMIC INVESTIGATIONS ALONG THE BUBU FAULT, DODOMA-TANZANIA

AS Macheyeke^(1,2,3,4), D Delvaux^(5,6), MD Batist⁽⁴⁾ and A Mruma⁽¹⁾

¹Geological Survey of Tanzania, P. O. Box 903, Dodoma, amacheyeke@yahoo.com

²School of Mines and Petroleum Engineering, The University of Dodoma, Tanzania

³Madini (Mineral Resources) Institute, P. O. Box 1696 Dodoma, Tanzania

⁴Renard Center for Marine Geology, Universiteit Gent, B-9000 Gent, Belgium

⁵Royal Museum for Central Africa, B-3080 Tervuren, Belgium

⁶School of Geosciences, University of the Witwatersrand, Johannesburg, South Africa

ABSTRACT

The central part of Tanzania, Dodoma, was hit by an $M_w = 5.5$ earthquake in November 4, 2002. It was part of a swarm of moderate earthquakes that affected the area. This paper, reports the first attempt to investigate significant past earthquakes along one of the known seismically active rift faults (Bubu fault, Gongga segment) by paleoseismological trenching. The trench revealed over 3 episodes of faulting (2 of which correspond to Mid-Holocene faulting). The magnitude of the largest earthquake illustrated in the trench is estimated at $M_w = 6.3-6.4$ and the slip rate between two recent faulting events is about 0.11 to 0.12 mm / yr. This shows that the Gongga segment of the Bubu fault is moderately tectonically active but seismically active of magnitudes of higher magnitudes.

Key words: Tanzania, Dodoma, Bubu fault, paleoseismic investigation, earthquake magnitude, slip rate, faulting.

INTRODUCTION

Earthquakes with magnitudes ranging from $M_w \leq 3.7$ to 5.5 have hit the northern part of Dodoma for many years (Iranga 1992, Nyblade and Brazier 2002, Macheyeke *et al.* 2008a, b). In 1994-1995, as shown by the data of the Tanzanian Broadband Seismic Experiment (Nyblade *et al.* 1996), and again in 2002-2003 (USGS data), it is clear that the earthquakes in the Dodoma area tend to occur in swarms. That last strong event culminated by the November 4, 2002, $M_w = 5.5$ earthquake that struck the Chenene Mountains, 80 km north of Dodoma Capital during a parliamentary session. Few people were reported dead, a school and a dispensary destroyed, and the old Tanzania parliamentary building located in Dodoma, cracked.

The Dodoma area is located in central part of Tanzania (Fig. 1) within the East African Rift System (EARS). It is characterized by at least seven active normal faults: the Mponde, Saranda, Bubu, Makanda, Hombolo, Bahi and Fufu faults (Macheyeke *et al.* 2009). Displacement profiles of these faults and their geometric patterns show that the faults are segmented, the length of each of the segments reflecting size of future earthquake potential for the given fault segments, with the highest value for the Gongga segment (Macheyeke *et al.*, 2009). Using 90 m resolution SRTM DEM data, and based on the empirical relationship of Wells and Coppersmith (1994), the first assessment of the seismic hazards in the Dodoma area by Macheyeke *et al.* (2009) showed that all these fault segments are able to generate earthquakes of magnitudes ranging between $M_w = 6.0 \pm 0.3$ to 7.0 ± 0.3 ,

assuming full reactivation of the given fault segment (Table 1). The ongoing seismicity, presence of Helium-bearing thermal springs and the occurrence of young fault systems with a fresh morphology (e.g. Shudofsky

1985, Iranga 1992, Macheyeke *et al.* 2009) show that the Dodoma area is a tectonically and seismically active portion of the EARS.

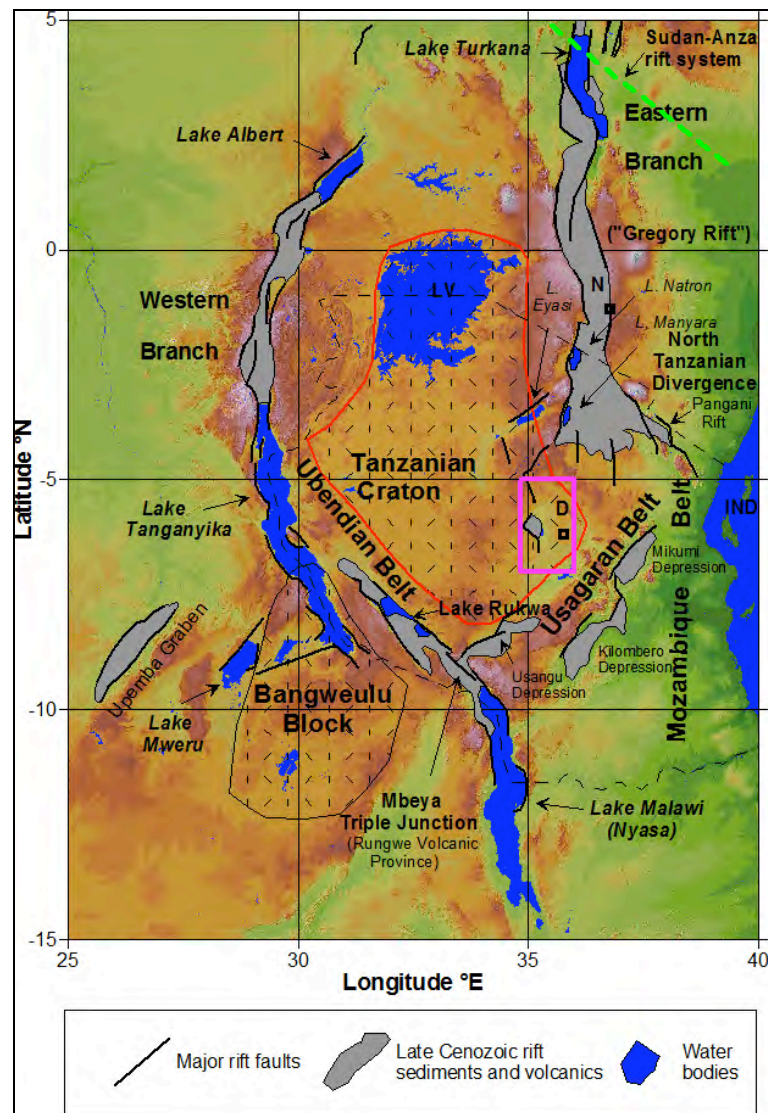


Figure 1: Schematic map of the EARS area. LV and IND stand for Lake Victoria and Indian Ocean respectively. D and N respectively stand for Dodoma and Nairobi. The study

area is shown by a pink rectangle. A red line represents the Tanzanian craton boundary (adapted from Delvaux 1991, Morley 1999, Macheyeki *et al.* 2008).

Table 1 List of faults in the Dodoma area along with their associated segments versus estimated possible maximum earthquake magnitudes (M_w) (Macheyeki, 2008), which can be generated by the fault segments. These estimates are only possible for each segment if and only if fully reactivation of each individual fault segment is attained (Wells & Coppersmith, 1994).

Fault / Fault segment	Fault length (km)	Maximum fault displacement (m)	Maximum magnitude of potential earthquake (M_w)
Mponde (Segment1)	31	1.41	6.8 ±0.3
Mponde (Segment2)	28	1.03	6.7 ±0.3
Saranda (Saranda south)	11	0.30	6.3 ±0.3
Saranda (Saranda mid)	29	1.41	6.8 ±0.3
Saranda (Saranda north)	24	1.03	6.7 ±0.3
Bubu (Nkambala)	33	1.41	6.8 ±0.3
Bubu (Makutupora)	30	~ 1.41	~ 6.8 ±0.3
Bubu (Gonga)	42	~ 2.62	~ 7.0 ±0.3
Hombolo / Dam	≥ 18	0.55 - 0.76	(6.5 - 6.6) ±0.3
Hombolo / Nzuguni	> 19	0.55 - 0.76	(6.5 - 6.6) ±0.3

In spite of these evidence, until now, no paleoseismic investigation was ever performed in the area, and therefore the presence of active faults has not yet been demonstrated. In order to fill knowledge gap, and improve our knowledge of the seismic potential of the Dodoma area in Central Tanzania, we performed a preliminary paleoseismic investigation to test if some of these faults present some Holocene activity. This work remains in a preliminary stage as only one trench has been dig and studied, but the results already demonstrate the occurrence of Holocene dislocation

Geological Setting

The Dodoma area is within the Dodoman tectonic domain that is part of the Tanzanian craton. The craton consists of granulated and sheared synorogenic granites as well as unsheared late-orogenic granites (Fig. 2). The whole rock radiometric dating of the

Tanzanian craton indicates that the ages of the migmatites and granitic complexes of the Dodoman tectonic domain range between 2.5 Ga to 1.87 Ga (Wendt *et al.* 1972, Gabert 1973, Gabert and Wendt 1974, Bell and Dodson 1981, Kabete *et al.* 2012). The Tanzanian craton is bounded to its eastern side by the Mozambique belt and the eastern branch of the East African rift develop in the pan-African suture zone (Tenczer *et al.* 2012) (Fig. 1). To the south, it is surrounded by remnants of the Paleoproterotoic Usagaran belt and the Central Tanzanian Shear Belt, strongly reworked or activated during the Pan-African orogeny (Pinna *et al.*, 2004, Vogt *et al.* 2006, Tenczer *et al.* 2007) (Fig. 2).

The Dodoma area is regionally characterized by folded structures with consistent ESE-WNW fold axes. These structures are thought to have developed during the Early Archaen Dodoman and Nyanzian orogenies

(Holmes 1952, Shackleton 1986). Pinna *et al.* (2004) showed the presence of E-trending thrust faults dipping northwards, south of the study area and NNE-SSW-trending thrust faults dipping eastwards along the eastern and northeastern cratonic magins. The late Cenozoic rift structures which develop in this area are controlled by this Precambrian Precambrian structural fabric (e.g. Fairhead and Stuart 1982, Macheyeke *et al.* 2008).

The Dodoma area remained stable for a long period after the Pan-African orogeny and was only destabilized during the development of the East African rift system, during which it gained its present elevation of ~ 1000 m above sea level. Rifting structure are not as well expressed as in the Kenya rift more to the north, but they are nevertheless representing the southwards continuation of the eastern branch of the East African rift system, after the North Tanzanian Divergence (Ebinger *et al.* 1997, Macheyeke *et al.* 2008, Delvaux and Barth 2010). The morphology of the central Tanzania plateau was driven by both the general elevation and block-faulting due to rifting. Just North of Dodoma, the large Bahi

depression formed between a series of normal faults of different orientation. The floor of this depression was largely covered during the Miocene - Early Pliocene by silcrete rich sandstones (Fawley 1956), known as the Kilimatinde Cement (Fozzard, 1961).

Site selection and trenching

The trenching site was selected on the basis of the seismo-tectonic activity, the morphostructural expression of the fault, the possible availability of datable material, the water table level, legal aspects, and the accessibility to the site.

As most faults in the Dodoma area are considered to be 'seismically active', we focused on those faults that are considered to present a medium to high likelihood for being reactivated under the present-day stress field by Macheyeke *et al.* (2008). Especially we selected both the Mponde and Bubu faults (Fig. 3) as they host an important number of thermal springs (e.g. James 1967, Walker 1969, Macheyeke *et al.* 2008).

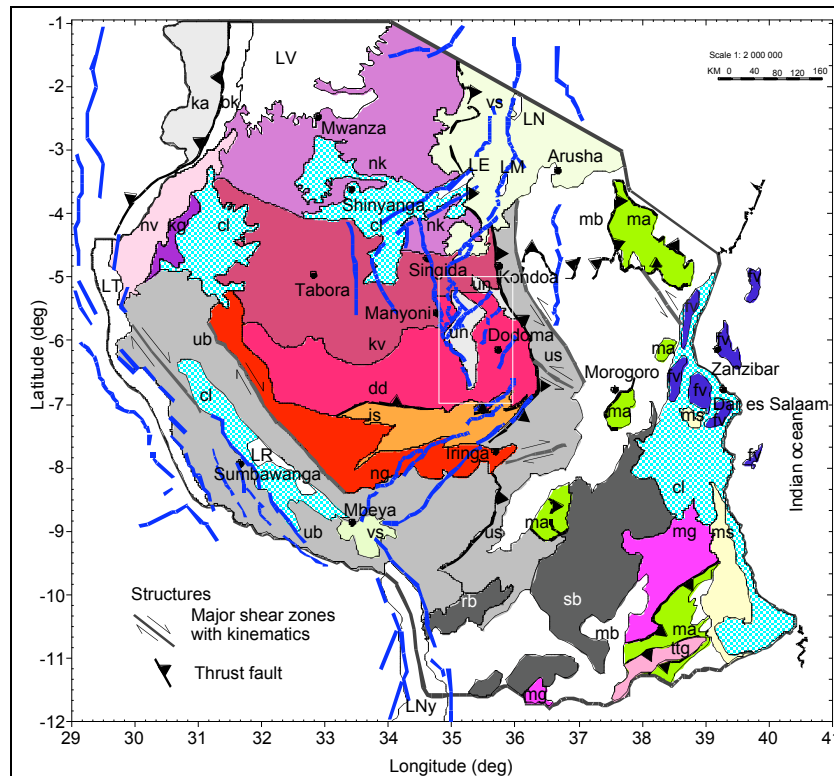


Figure 2 CENOZOIC FORMATION **un** = undifferentiated Neogene to Quaternary continental sedimentary formations; **cl** = continental and lacustrine sedimentary formations; **vs** = Neogene-Quaternary volcanic formations; **fv** = Paleogene-Neogene sediments: marine, lacustrine and fluvio-marine formations. PALEOZOIC and MESOZOIC BASINS: **ms** = cretaceous sediments: marine and continental formations (sandstone, conglomerate); **rb** = Karoo formations in the Ruhuhu basin; **sb** = Karoo formations in the Selous basins. NEOPROTEROZOIC DOMAINS: **bk** = Neoproterozoic to Cambrian detrital sediments: Manyovu Red Beds, Ikorongo group; **nv** = Neoproterozoic volcano-sedimentary formations: Uha group, Nyamori Supergroup; **kg** = Neoproterozoic sedimentary formations (Kigonero Flags Group, Nyamori Supergroup, formerly known as Bukoban Sandstone); **mb** = Mozambique belt; **ma** = Neoproterozoic high-grade mafic and felsic granulite, gneiss and migmatite granulite-facies metamorphism, interlayered with amphibolite, marble, quartzite, schist and mylonite. MESOPROTEROZOIC DOMAINS: **ttg** = Mesoproterozoic-Neoproterozoic Tonolite Trondjemite Granitoids and migmatites; **mg** = Mesoproterozoic orthogneiss (ca. 1.19-0.0945 Ga) affected by Neoproterozoic high-grade metamorphism (Songea and Kimambi groups); **ka** = Mesoproterozoic Karagwe-Ankolean detrital metasediments (≥ 1.37 Ga). PALEOPROTEROZOIC DOMAINS: **ub** = Ubendian belt; **us** = Usagaran belt. ARCHEAN BASEMENT: **ng** = Neoproterozoic granitoid; **nk** = Neoproterozoic TIG granitoid and sediments (Nyanzian and Kavirodian Supergroups); **kv** = Neoproterozoic-Undifferentiated granitoid, migmatite, mafic and ultramafic rock: sediments of the Kavirodian Supergroup; **dd** = Dodoman Group (ca. 2.90-2.50 Ga); **is** = Isangani group (ca. 3.0-2.85 Ga). BODIES: **LV** = Lake Victoria; **LT** = Lake Tanganyika; **LR** = Lake Rukwa; **LNy** = Lake Nyasa; **LE** = Lake Eyasi; **LM** = Lake Manyara; **LN** = Lake Natron (Modified after Pinna *et al.* 2004).

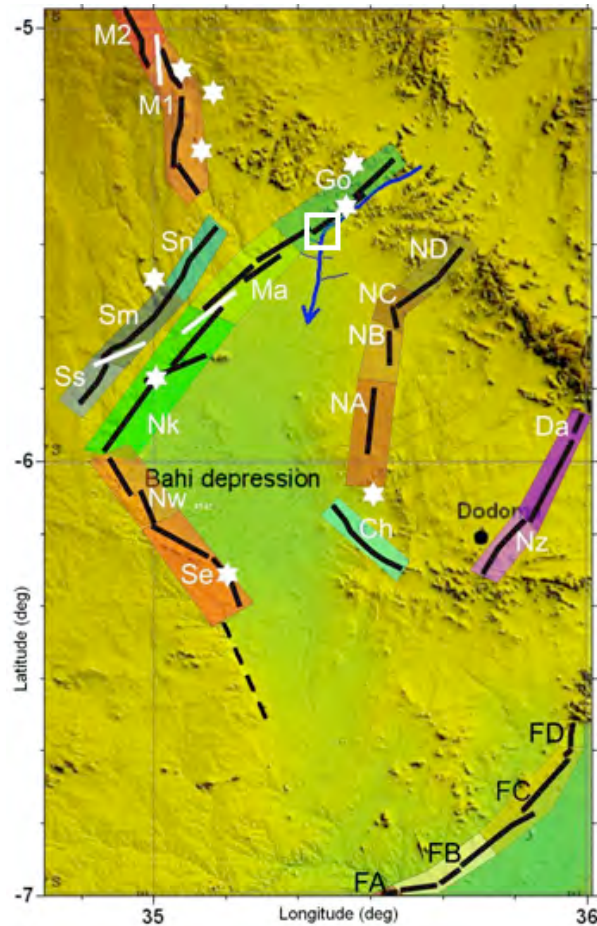


Figure 3: Fault segments as computed from data extracted from 90 m resolution SRTM-DEM. Mponde fault: M1 = Segment 1, M2 = Segment 2. Saranda fault: Ss = Saranda south segment, Sm = Saranda mid segment, Sn = Saranda north segment. Bubu fault: Nk = Nkambala segment, Ma = Makutupora segment, Go = Gonga segment. Bahi fault: Nw = Northwestern segment, Se = Southeastern segment. Makanda fault: NA = Segment A, NB = Segment B, NC = Segment C, ND = Segment D. Hombolo fault: Nz = Nzuguni segment, Da = Dam segment. Fufu fault: FA = Segment A, FB, Segment B, FC = Segment C, FD = Segment D. Chikola fault: Ch = Chikola. White stars represent locations of thermal springs and white lines represent relay ramps that were studied in detail. Black lines are faults (fault traces). Box on Gonga segment represent an area in which the Magungu trench was established.

The Bubu fault was preferred as it presents a morphology that is more favorable for paleoseismic investigation, following the criteria of Dost and Evers (2001). The trench was established at Magungu (35°20'36"E/5°28'51"S, Arc 1960).

The trench was established at the base of a nearly 90 m higher fault scarp (Fig. 4, 5a) whose topmost part (footwall side) fairly tilts due east. The trench site (hanging wall side) slopes gently to the east at 10 - 15°. It

is covered by relatively thick loamy sandy soils. Few angular boulders occur as floats in the area. Two sub parallel streams “R” and “Q” occur to the northern side of the trench and a third one “P” to the southern part. All the three streams are tributaries to the Bubu River located few kilometers east of the trench site. Based on a topographic profile of the Magungu area that was

established about 100 m NE of the Magungu trench (offset due to thick tree cover) the trace of the trench is projected as on Figure 5b. The height of this scarp is undoubtedly a result of long term multiple faulting activities most likely since Mid-Late Pleistocene (~ 1.3-1.2), during the second-rifting stage (e.g. Fairhead *et al.* 1972, MacIntyre *et al.* 1974)

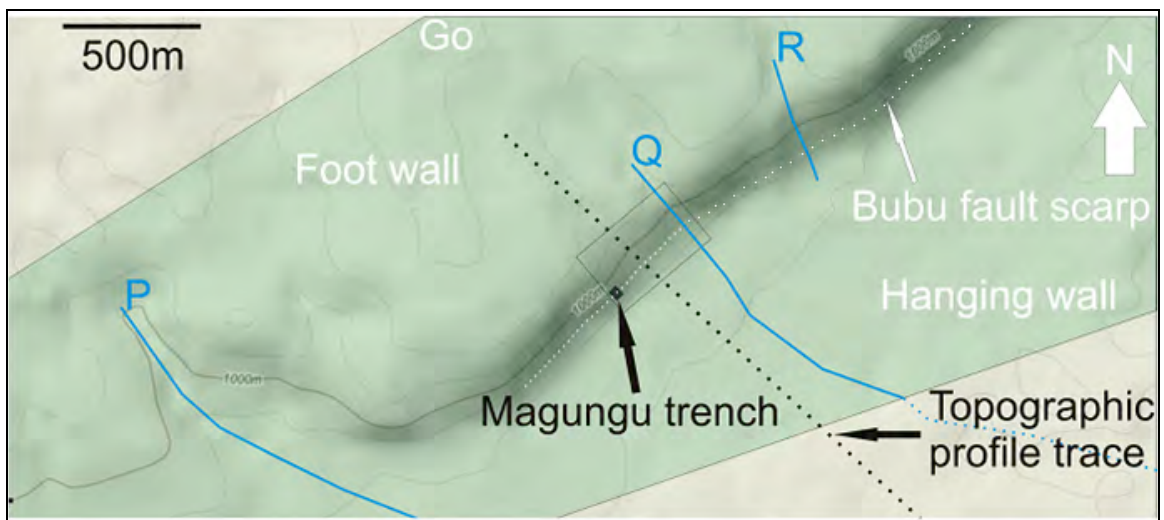


Figure 4: The detailed topographic map of the Gongga segment (Go) at Magungu trench within the 90 m resolution SRTM-DEM with 50 m contour lines. Blue lines are tributaries P, Q and R of the Bubu River that is found on the eastern side of this map. Blue dotted lines are inferred trace of the tributary ‘Q’. The trench was established around 960 m above the sea level. The rectangle in thin black outline points the location of the picture in Fig. 5.



Figure 5a Front view of Gongga segment scarp at Magungu village. Arrow points the location of the Magungu trench.

Trenching

The Magungu trench was excavated on either side of scarp base marked by the slope inflexion point, intersecting both the hanging wall and footwall (Fig. 5b, 6). It was dug perpendicular to the fault, wider and long enough to allow easy trenching,

logging and sampling. The trench floor was leveled by excavating from the bottom of trench on the hanging wall side (as a reference level) towards the footwall side. The trench is 11 m long, 1.5 m wide and 4 m deep; it is oriented 320°.

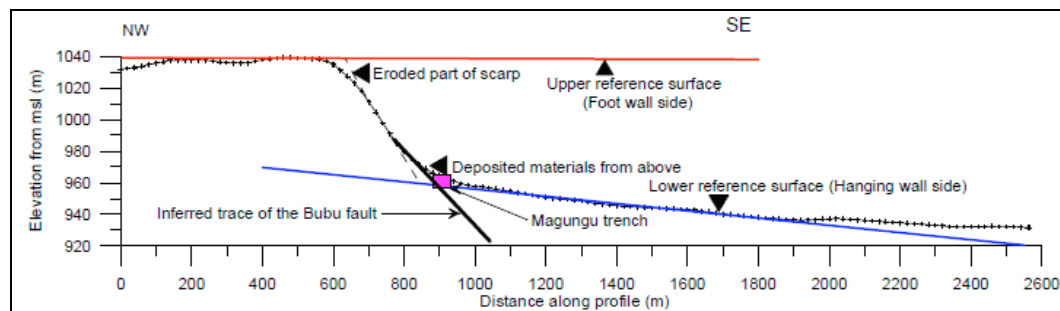


Figure 5b The topographic profile of the Bubu fault at Magungu showing the approximate location of the Magungu trench. In Fig. 4, the trace of this topography is shown by a dashed black line drawn perpendicular to the fault. Note also that the trench location is projected about 100 m NE from its location. Compare the location and elevation of the trench from Fig. 5a.



Figure 6 Picture of the Magungu trench as seen from the hanging wall side. Picture taken facing N320⁰W (the orientation of the trench). The white line represents approximate inflexion point.

Gridding

A local grid was established on the southwestern wall, where most deposits or units and structures or faults have been preserved, gridded in 2 x 2 m and leveled using a water filled flexible pipe. The horizontals and verticals were marked by a rope nailed into the trench wall and labeled.

Sampling and radiocarbon dating

Three samples were taken for ¹⁴C dating; MAG01, MAG02 and MAG03 (Fig. 7a, b). Samples MAG01 and MAG02 are from layer C3b and MAG03 is from layer KC; details of which are given in section 4. A knife was used to snatch fine materials from the trench wall into small labelled plastic bags which were then air freed and covered

ready for submission to a laboratory for analysis.

Radiocarbon dating was done using 14-C Accelerator Mass Spectrometer on organic carbon residue from the sediment in accordance to the procedures at the University of Utrecht (R. J. Van de Graaff laboratorium). The Calibration to Calendar age (cal. BP) interval corresponds to 1 σ (68% confidence level).

Trench description

At least 5 different lithologic units were revealed in the trench as described below (Figs. 7-9).



Figure 7a: Photograph mosaics of the SW wall of the Magungu trench. The pictures are a little bit distorted because they were taken at different positions and at slightly different orientations.

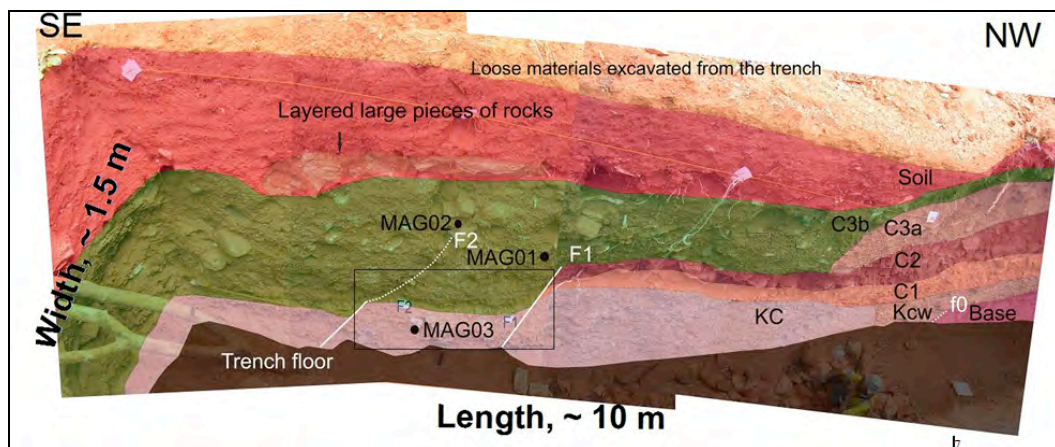


Figure 7b Interpretation of the Magungu trench. Photographs taken facing the southwestern wall (with part of the southeastern part or width part) of the Magungu trench. 'Bas' stands for basement. Rectangle 'a' is represented by a corresponding 'zoom in' of the same stratigraphic unit on the opposite wall rotated 180° (Fig. 8). An area defined by rectangle 'b' is magnified in Fig. 9. Sample points as black dots and sample numbers MAG01; MAG02 and MAG03 are also shown. Fig. 10 carries the similar information into scale.

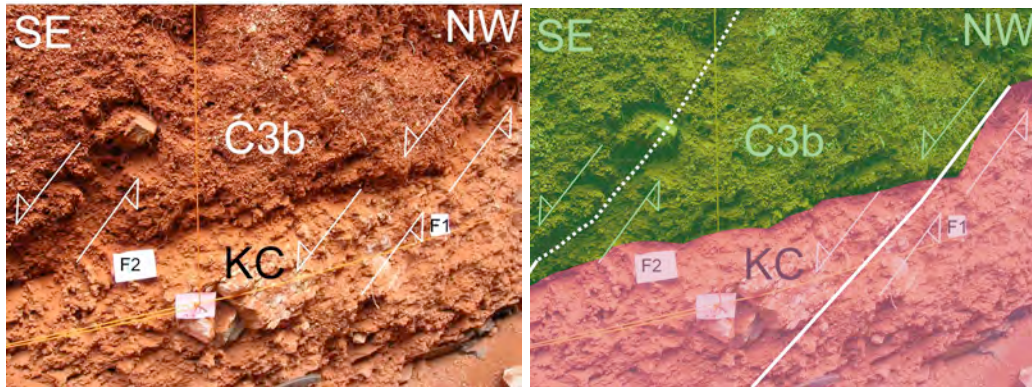


Figure 8: A zoom in on the rectangle ‘b’ in Fig. 7b. In this picture, the most recent faults, F1 and F2 and their kinematics are shown. Left: A necked picture, Right: the same as left but with boundaries of units C3b and KC drawn. Locations of faults F1 and F2 are also shown by white lines. The dashed line part of F2 implies that part of F2 is not very certain (Compare with Figs. 7, 9).

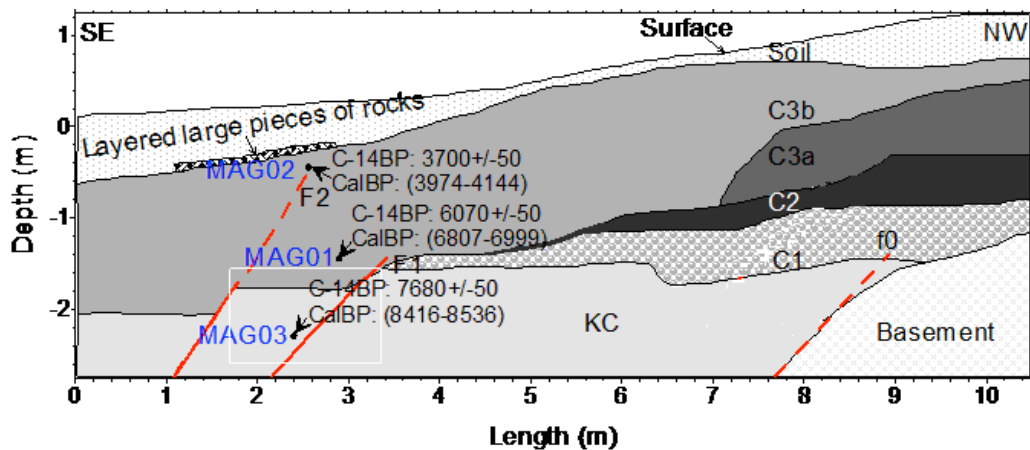


Figure 9: Interpretation of the Magungu trench cross-section showing various deposits which are displaced in parts by normal faults, F1 and F2. The white rectangle ‘a’ is the same as in Fig. 7b. We add the calibrated 14C - ages of MAG01, MAG02 and MAG03 as well. The local coordinates of the samples (x, y) are: MAG01 = (2.89, -1.45), MAG02 = (2.55, -0.45) and MAG03 = (2.38, -2.24); all coordinates in meters as shown in the figure.

Basement. The basement is exposed over 200 cm in the hanging wall side. It is a highly to moderately weathered gneiss and intercalated by mafic rocks of unknown origin. The basement is thought to be cut by a normal fault (f0). The fault f0 is

considered to be an oldest fault intersected in the trench. It dips $\leq 40^\circ$ towards SE. The approximate position of f0 was established based on the fact that it is at this place where the basement outcrops as a highly weathered

unit. At this place, the basement is also in contact with a highly weathered unit 'KC'.

Unit KC. This unit that is mainly a hard substance is coherently calcrete-rich with reddish cemented silt-sand matrix. In contact with and close to the basement, KC is highly weathered and intercalated with weathered basement fragments. Unit KC overlies the basement unconformably. It has a thickness of over 100 cm and it is cut by two normal faults F1 (45°SE) and F2 (54°SE) towards the foot of scarp and partly by f0. The fault planes of F1 and F2 are not associated with slip lines.

Unit C1. Like Unit KC, Unit C1 is also in contact with the basement. It consists of loose conglomeratic materials that are characterized by rounded to sub-rounded basement gneiss pebbles of up to 15 cm in diameter. It has a thickness of up to 80 cm and thins away towards both the hanging wall and footwall. The unit tapers off progressively on the hanging wall side and appears to be truncated by F1 as it comes in contact with KC and C3.

Unit C2. This unit has a thickness of up to 60 cm. It is a clast supported and consists of unsorted angular pebbles and boulders that are randomly deposited. It also has a significant amount of pisoliths and unconformably overlies C1.

Unit C3a. This unit consists of reddish brown colluvium characterized by a matrix supported materials that are unsorted angular pebbles and boulders with pisoliths. Unlike C2, angular pebbles and boulders in C2 are relatively fewer and they are relatively more weathered than those in C2. It is up to 70 cm thick. It overlies C2 unconformably. Its upper contact with C3b is relatively diffuse and its texture and extent are not so distinct.

Unit C3b. This unit consists of reddish brown colluvium with unsorted sub angular

gravel, pebbles and soil. Roots from dead trees and grasses are common. It is over 100 cm thick and extends on both the hanging wall and footwall sides outside the trench limits. It covers unconformably all units C2, C1 and KC. It is cut, in parts, by both F1 and F2. F1 has a displacement of about 35 cm and F2 has a displacement 30 cm. These displacements are along the fault planes. MAG01 was taken in order to constrain the age limit of F1 and the maximum age of C3b. Similarly, MAG02 was taken in order to constrain the lower limit ages of both C3b and an inferred fault F2. For the age of KC, MAG03 was taken.

INTERPRETATION AND DISCUSSION

Here we describe briefly our interpretation of various lithologic units vs. tectonic activities with time. We also discuss potential earthquakes and finally we discuss geomorphic indicators.

Sequence of events

Both relative and absolute chronostratigraphy in the context of active faulting have been given in this sub-section.

The oldest faulting phase, f0 seems to affect both the basement and KC, but the amount of displacement is not clear (Figs. 7, 9). The deposition of the conglomeratic unit C1 above KC is interpreted as reflecting the onset of a high energy environment as a consequence of vertical differential movement, but with a distal source due to size and roundness of deposits. Unit C2 with angular blocks corresponds to a more proximal source. Emplacement of C2 on top of C1 with a sharp contact could have been triggered by an unknown faulting event not visible here. Unit C3a deposited on top of C2 contains finer but still angular rock fragments.

Unit C3 was deposited discordantly above KC, C2 and C3a with a relatively sharp contact, overlapping the previous units.

Fault F2 was active during the deposition of C3b, F1 occurred earlier than F2. F1 is displacing the basal contact of C3b. F2 is also displacing the basal contact of C3b but in a more sharp way and it is seen to affect most of the C3b profile. The youngest deposit in the sequence (soil) is not affected by any faulting displacement (Fig. 7, 9).

The successive events illustrated in the Magungu trench can be summarized as follows: (1) The calcareous - rich (with silcretes) material KC is faulted against the basement along fault f0, (2) a relatively distal differential vertical movement induced deposition of the conglomerate C1, (3) more proximal movements brought the angular pebbles and boulders of Unit C2, (from an unknown source), (4) reddish brown colluvium (Unit C3b) is covering indifferently the former deposits during the development of F2, (5) the whole structure is covered by the superficial soil which means that the youngest deposit in the

sequence is soil. Therefore, the whole relative age of faults and stratigraphic or lithologic units relationship can be summarized as; Basement → KC → ?f0 → regional easterly tilt + erosion → C1 → C2 → C3a → F1 → C3b → F2 → Soil.

The ¹⁴C-ages obtained are as follows: as stated above, MAG01 and MAG02 were taken in order to constrain Unit C3b. MAG01, which was taken close to the bottom of Unit C3b but just above the horizon truncating F1, yielded an age of 6807-6999 cal. yr BP, while MAG02, close to the summit of Unit C3b, supposedly above the event horizon related to F2, yielded an age of 3974-4144 cal. yr BP. Thus, event 3 (Table 2) is bracketed between MAG02 (minimum) and MAG01 (maximum), and events 2 and 1 are bracketed between MAG01 (minimum) and MAG03 (maximum).

Table 2: The list of observed faults in the Magungu trench and their possible relative age. VO stand for vertical offset (displacement, in cm) and M_w stands for Potential earthquake magnitude in M_w.

Fault	VO	M _w	Overall slope angle (°)	Relative age within the trench
f0	??	Not easy to establish	≤ 40	Probably the oldest fault
F1	35	≤ 6.4	45	Younger fault
F2	30	6.3	54	Youngest fault

For unit KC, sample MAG03 was taken and yielded an age of 8416-8536 cal. yr BP. Thus unit KC is much younger than it was thought before. Previously, we considered KC to be the Kilimatinde Cement, i.e. of Miocene to Early Pliocene age. Our assumption was based on the texture of the deposit, the composition of the deposit (calcrete-rich) and its relationship with the basement, i.e. it overlies the basement (e.g. Fozzard 1961). Therefore, we then take this

age interval, i.e. 8416-8536 cal. yr BP to be the minimum age of unit KC and maximum age of F1 (Table 3).

The absolute dating does not allow separating events 1 and 2, although they appear to be stratigraphically separated. To calculate the interval between events 2 and 3, the full age brackets for both events have to be considered, yielding a minimum age of 6807-6999, which is negative (-192yr) and

thus becomes 0, and a maximum age of 4562 yr (8536-3974).

Table 3:

Faulting event	Minimum age (cal. yr. BP)	Maximum age (cal. yr. BP)
Event 3 (on splay F2)	3974 - 4144	6807 - 6999
Event 2 (on splay F1)	6807 - 6999	8416 - 8536
Event 1 (on unknown fault)	6807 - 6999	8416 - 8536

Using the full probability density function, instead of just the 1- σ age values we obtain 2- σ age values as shown in Fig. 10. Note that the scale for the two upper plots is absolute age (in calibrated years BP), whereas the scale for the lower plot is time span (in years). The top plot shows the calibrated ages of the three samples, MAG01, MAG02 and MAG03. The middle plot shows the probability density functions for events 3 and 2 (and for event 1 as well,

since event 1 has the same bounds as event 2). The lower plot shows the probability density function for the interval between events 3 and 2.

From Fig. 10, the probability density function for the interval between event 3 and 2 ranges between 0 and more than 4000 years, although the probability that it is 0 is less than that it is along the horizontal axis (time span in years).

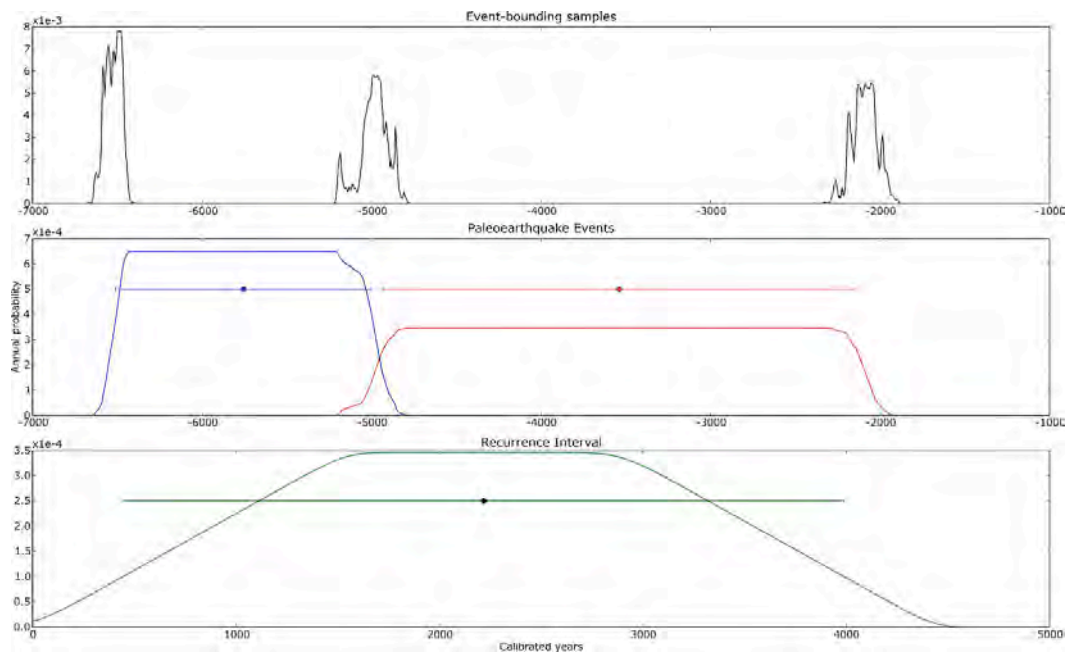


Figure 10: The 2- σ value plots for the three samples MAG01, MAG02 and MAG03 using the full probability density function.

Thus we obtain the following 2- σ ranges:

Event 3: -4926.9 to -2143.6 (Mean: -3539.7)

Event 2: -6505.8 to -4998.8 (Mean: -5754.7)

In other words, the interval 1 (i.e. the range between event 3 and event 2) corresponds to the whole range from 444.6 yr to 3989.4 yr (Mean: 2216.9 yr). Thus, recurrence interval corresponding to 2- σ probability = 2216.9 yr.

These results also show that the most recent tectonic activity (F2) took place in the Middle Holocene (more recent than 6807-6999 cal. yr BP), Fig.9).

Using $RI = D / (S-C)$, where RI is the mean recurrence interval, D is the displacement during a single, typical faulting event, S is the coseismic slip rate, and C is the creep slip rate (assumed to be zero for most faults unless historic creep has been documented), then the corresponding average coseismic slip rate between the two discrete events F1 and F2 is

$(35+30)/2 \text{ cm}/2216.9 \text{ yr} = 0.014660 \text{ cm / yr}$
or 0.15 mm/yr.

However, this slip rate is just tentative as three age data points cannot provide a statistically sound recurrence interval (or slip rate).

Paleoearthquake magnitudes

Using the empirical relations between vertical offset and maximum magnitudes (e.g. Wells & Coppersmith, 1994), the amount of displacement or vertical offsets in faults revealed in the Magungu trench reflects the magnitudes of paleoearthquakes. Faults F1 and most likely F2, are assumed to be associated with paleoearthquake events and they clearly reflect large (destructive) earthquakes with magnitudes of the order of $M_w = 6.3$ to 6.4 (Table 1).

Reasoning in the same lines, we can therefore expect potential future earthquakes

of the order of M_w 6.3 to 6.4 to be generated by the Gongga segment. However, at this stage a question builds up in one's mind as to why should there be a difference between these paleoseismologically derived M_w values from those reported in Macheyeki *et al.*, (2008; 2009) which were computed from SRTM-DEM data on the same fault segment? The latter are higher than the former by about $M_w = 0.6$ which corresponds to an earthquake magnitude of about 6x or more in terms of energy generated. There are two possible explanations for this discrepancy. The first one is that, the Magungu trench in this study, was not able to reveal all the recent faults due to its limited lateral extend and depth. The second one is that the Gongga segment might be having (and most likely so) some small satellite faults that form it, thus, the Magungu trench was established in one of these satellite faults. The third one is the presence of a NW-SE trending Maziwa fault that runs between the Bubu and the Makanda fault (Fig. 3) could also be considered as a fault that transfers deformation / and stress between the two faults and hence acts a buffering system. The buffering system could explain a value of magnitude lower than predicted by Macheyeki *et al.* (2008, 2009).

Geomorphic indicators

Based on the presence and position of a conglomeratic unit (C1) in the trench (Figs. 7, 8-9, 10), this, as stated earlier, represents both high energy environment source and long distance travel of clastic materials most likely by water before deposition. As per Macheyeki *et al.* (2008), the regional tilt is reported to affect all major faults in the area and can also be clearly revealed on the geomorphology of the whole study area (Fig. 8, see Fig. 9 for location of section). We therefore consider the regional tilt to be post main faulting event in the area.

CONCLUSION AND RECOMMENDATIONS

We have been able to demonstrate that a minimum total of 5 major tectonic event have affected the Bubu fault (Gonga segment). These are, listing chronologically from oldest: (1) quite environment, (2) regional easterly tilt associated with erosion, (3) quite environment, (4) normal faulting associated with large earthquakes and (5) quite environment at present that gives room to soil cover development. This pattern is undoubtedly a time dependent, i.e. repeats itself at some intervals which have not yet to be determined.

To our understanding, this paleoseismic investigation is a first attempt performed in the the Dodoma area. Although the data are limited in number, yet, together with the study of both geomorphic and stratigraphic indicators, they suggest that the area is prone to future large earthquakes larger than the November 2002. More work is needed to confirm and detail this finding. If confirmed, any infrastructures such as road bridges, tall buildings to be built on this area must be able to withstand large earthquakes of more than 8x larger than that of November 4, 2002.

ACKNOWLEDGEMENT

This work is being supported by Belgium Technical Cooperation and the Government of the United Republic of Tanzania. We are indebted to S. Abel from the Mineral Resources Institute in Dodoma for his technical assistance in the field. F. Kervyn from the Royal Museum for Central Africa is highly appreciated for the processing of the 90 m SRTM - DEM data. K. Verbeeck and T. Petermans from the Royal Observatory of Belgium are highly appreciated for their constructive comments. Similarly, we thank Audray Delcamp from Vrije Universiteit Brussel. Many thanks to anonymous reviewers

REFERENCES

- Barth H, 1996 Gold in the Dodoman basement of Tanzania, pp.1-53, Hanover.
- Bell K, Dodson HS, 1981. The Geochronology of the Tanzania Shield. *J. Geol.* **89**(1): 109-128, Chicago.
- Delvaux D, Barth A, 2010 African Stress Pattern from formal inversion of focal mechanism data. Implications for rifting dynamics. *Tectonophysics* **482**: 105-128.
- Dost, B., Evers, L., 2001. Paleoseismology: in search of large earthquakes, Climate Research and Seismology-Biennial Report, 2001.
- Ebinger C, Poudjom Djomani Y, Mbede E, Foster A, Dawson JB, 1997 Rifting Archaean lithosphere : the Eyasi-Manyara-Natron rifts, East Africa. *J. Geol. Soc. London* **154**: 947-960.
- Fairhead JD, Mitchell JG, Williams LAJ, 1972 New K/Ar determinations on Rift volcanics of South Kenya and their bearing on the age of Rift faulting. *Nature* **238**: 66-69.
- Fairhead JD, Stuart GW, 1982 The seismicity of the East-African rift system and comparison with other continental rifts. In: Palmason, G. (ed.): Continental and Oceanic Rifts. *Geodynamic Series* **8**: 41-61.
- Fawley AP, 1956 Diamond drilling in the Bahi Swamp. Records of the Geological Survey of Tanganyika **6**: 47-51.
- Fozzard PMH, 1960 Geological Survey of Tanzania. 1:125.000 Geological map Quarter Degree Sheet 124 Kelema. Geological Survey Division, Dodoma.
- Fozzard PMH, 1961 Geological Survey of Tanzania. 1:125.000 Geological map Quarter Degree Sheet 123 Kwa Mtoro. Geological Survey Division, Dodoma.
- Fozzard PMH, 1962 Brief explanation of the Geology of QDS177 Manzoka- Geological Survey of Tanganyika, pp. 1-7, Unpublished Report, Dodoma.
- James TC, 1967 Thermal springs in Tanzania. Institution of Mining and Metallurgy, Transactions/Section B

- (Applied earth science) 76, B1-18.
- Julian W, Lounsberry W, Tamura A, Van Loenen R, Wright MP, 1963 Geological Survey of Tanzania 1:125,000 Geological map Quarter Degree Sheet 143 Meia Meia. Geol. Survey Division, Dodoma.
- Kabete JM, Groves DI, McNaughton NJ, Mruma AH, 2012 A new tectonic and temporal framework for the Tanzanian Shield: Implications for gold metallogeny and undiscovered endowment. *Ore Geol. Rev.* **48**: 88-124.
- Lounsberry W, Van Loenen R, Wright MP U.S.A. Peace Corps 1963 and Haslam, H. W., 1967. Mineral Resources Division, Tanzania. 1:125.000 Geological map Quarter Degree Sheet 142 Bahi. Geological Survey Division, Dodoma.
- Macheyeki AS, Delvaux D, De Batist M, Mruma A 2008 Fault kinematics and tectonic stress in the seismically active Manyara-Dodoma rift branch in Central Tanzania - Implications for the East African Rift. *J. Afr. Earth Sci.* **51**(4): 163-188.
- Macheyeki AS, Delvaux D, De Batist M, Mruma M 2009 Active faults and fault segmentation in the Dodoma area, Tanzania: A first assessment of the seismic hazard in the area. *Tanz. J. Earth Sci.* **1**: 38-57.
- MacIntyre RM, Mitchell JG, Dawson JB 1974 Age of the fault movements in the Tanzanian sector of the East African rift system *Nature* **247**: 354-356.
- Nyblade AA, Birt C, Langston CA, Owens TJ, Last RJ, 1996 Seismic experiment reveals rifting of craton in Tanzania, *Eos Transac. AGU* **77**: 517-521.
- Shudofsky GN, 1985 Source mechanisms and focal depths of East African earthquakes using Raleigh-wave and body wave modeling. *Geophys. J. Royal Astronomic. Soc.* **83**: 563–614.
- Tenczer V, Hanzenberger Ch, Fritz H, Hoinkes G, Muhongo S, Klötzli U, 2012 Crustal age domains and metamorphic reworking of the deep crust in Northern-Central Tanzania: a U/Pb zircon and monazite age study. *Mineralogy and Petrology*. DOI 10.1007/s00710-012-0210-1.
- Vogt M, Kröner A, Poller U, Sommer H, Muhongo S and Wingate MTD, 2006 Archaean and Palaeoproterozoic gneisses reworked during a Neoproterozoic (Pan-African high-grade event in the Mozambique belt of East Africa: Structural relationships and zircon ages from Kidatu area, central Tanzania. *J. Afr. Earth Sci.* **45**(2): 139-155.
- Wades FB, Oates F, 1938 An explanation of degree sheet no. 52, Dodoma, *Geological Survey of Tanganyika*. **17**: 1-60, Dar es Salaam.
- Walker BG, 1969 Springs of Deep Seated Origin in Tanzania. *Proceedings of the XXIII International Geological Congress* **19**: 171-180.
- Wells DL, Coppersmith KJ, 1994 New empirical relations among magnitude, rupture length, rupture width, rupture area and surface displacement. *Bull. Geol. Seism. Soc. Am.* **84**: 974-1002.